Author's Accepted Manuscript

www.elsevier.com/locate/memsci

Attrition-resistant membranes for fluidized-bed membrane reactors: double-skin membranes

Alba Arratibel, Jose Antonio Medrano, JonMelendez, D. Alfredo Pacheco Tanaka, Martin van Sint Annaland, Fausto Gallucci

PII: S0376-7388(18)30962-1
DOI: https://doi.org/10.1016/j.memsci.2018.06.012
Reference: MEMSCI16229

To appear in: *Journal of Membrane Science*

Received date: 9 April 2018
Revised date: 31 May 2018
Accepted date: 6 June 2018

Cite this article as: Alba Arratibel, Jose Antonio Medrano, Jon Melendez, D. Alfredo Pacheco Tanaka, Martin van Sint Annaland and Fausto Gallucci, Attrition-resistant membranes for fluidized-bed membrane reactors: double-skin membranes, *Journal of Membrane Science,* https://doi.org/10.1016/j.memsci.2018.06.012

Attrition-resistant membranes for fluidized-bed membrane reactors: double-skin membranes

Alba Arratibel[1,2], Jose Antonio Medrano[1], Jon Melendez[2], D. Alfredo Pacheco Tanaka[2], Martin van Sint Annaland[1], Fausto Gallucci[1,*]

[1] Department of Chemical Engineering and Chemistry, Eindhoven University of Technology (TU/e), Den Dolech 2, 5612AD, Eindhoven, The Netherlands

[2] TECNALIA, Membrane Technology and Process Intensification, Mikeletegi Pasealekua 2, 20009, San Sebastian-Donostia, Spain

ABSTRACT

Pd-Ag supported membranes have been prepared by coating a ceramic interdiffusion barrier onto a Hastelloy X (0.2 μm media grade) porous support followed by deposition of the hydrogen selective Pd-Ag (4-5 μm) layer by electroless plating. To one of the membranes an additional porous Al_2O_3-YSZ layer (protective layer with 50 wt% of YSZ) was deposited by dip-coating followed by calcination at 550 °C on top of the Pd-Ag layer, and this membrane is referred to as a double-skin membrane. Both membranes were integrated at the same time in a single reactor in order to assess and compare the performance of both membranes under identical conditions. The membranes have first been tested in an empty reactor with pure gases (H_2 and N_2) and afterwards in the presence of a catalyst (rhodium onto promoted alumina) fluidized in the bubbling regime. The membranes immersed in the bubbling bed were tested at 400 °C and 500 °C for 115 and 500 hours, respectively. The effect of the protective layer on the permeation properties and stability of the membranes were studied. The double-skinned membraned showed a H_2 permeance of $1.55 \cdot 10^{-6}$ mol m^{-2} s^{-1} Pa^{-1} at 500 °C and 4 bar of pressure difference with an ideal perm-selectivity virtually infinite before incorporation of particles. This selectivity did not decay during the long term test under fluidization with catalyst particles.

Graphical abstract:

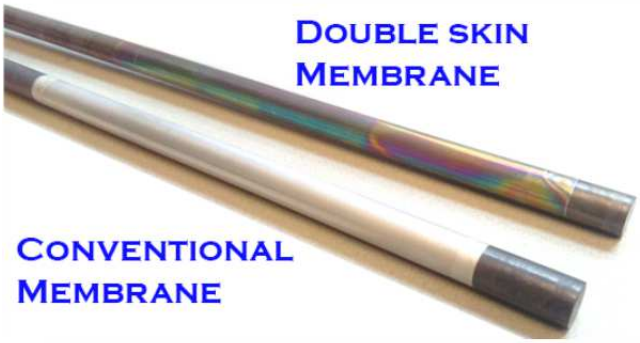

Keywords: Pd membranes, double-skin, hydrogen separation, fluidized beds

Corresponding author: F.Gallucci@tue.nl

1. Introduction

The steam methane reforming (SMR) process is the conventional, and currently most cost effective, technology for hydrogen production at large scale [1]. In this process, the methane is converted at high temperatures (around 900 °C) into hydrogen in a reformer reactor, which consists of fired multi-tubular fixed bed reactors filled with, commonly, Ni-based catalysts [2]. The reaction is limited by the thermodynamic equilibrium and is also highly endothermic which results in a highly energy-intensive process. The syngas produced in the reformer is subsequently fed to water gas shift reactors for further fuel conversion and the hydrogen produced is separated at low temperatures by pressure swing absorption (PSA) [3]. Hydrogen is normally consumed in the chemical industry for ammonia and methanol production, and in hydrocracking processes in oil refineries. Nowadays, hydrogen also finds application for power generation in fuel cells, where high purities (>99.99 %vol.) are required [4].

In the last years, new technologies have been proposed in order to improve the reforming efficiencies for hydrogen production. Membrane reactors represent an evolution of the reformer, where H_2 perm-selective membranes are immersed in the catalytic reaction zone and remove, in-

situ, the produced hydrogen, thus yielding higher fuel conversions owing to the shifting of equilibrium conditions. The continuous selective separation of hydrogen allows operation at much lower operating temperatures, which decreases the energy consumption of the highly energy-intensive process [5,6]. Additionally, the reactor volumes are reduced and downstream conversion and hydrogen separation processes are circumvented. Different membrane reactor configurations have been proposed and demonstrated in the literature for hydrogen production using methane as feedstock. In particular, fixed/packed bed and fluidized bed membrane reactors are the ones more investigated in the open literature. In general, it is well accepted that fluidized bed membrane reactors (FBMR) can provide improved heat and mass transfer, and lower pressure drop compared to packed bed reactors.

Palladium-based membranes offer the capacity to extract high fluxes of hydrogen based on the high permeability of Pd and its alloys (Ag, Cu, Au…) with high perm-selectivities. In order to increase the hydrogen fluxes through the membrane and, simultaneously decrease the membrane costs while maintaining the membrane mechanical strength, the deposition of very thin Pd-layers onto porous supports is generally the only industrially viable route. To achieve defect-free thin layers on top of porous substrates, low surface roughness and small pore sizes (with narrow pore distribution) of the support materials are required [7]. On the one hand, ceramic supports (Al_2O_3, ZrO_2, YSZ, etc.) are the most exploited so far, due to their high chemical stability, low cost and high surface quality. However, their mechanical strength is lower compared to metallic supports and the sealing of such supports in membrane modules is more challenging [7]. On the other hand, metallic supports provide a much higher mechanical strength and relatively easy integration into a reactor. However, their surface quality is generally lower. The relatively large roughness and pore size (2-20 μm) of metallic supports can be reduced by the deposition of a ceramic porous layer, which also helps avoiding inter-metallic diffusion of elements present in the metallic support and the Pd-based selective layer, when the membranes are employed at high temperatures under reducing environments. Ceramic barriers have been successfully deposited onto metallic supports by dip-coating [8–12], sputtering [13–15] and atmospheric plasma deposition (APS) [13,16,17]. Prior to the deposition of the ceramic barrier, a heat treatment of the metallic stainless steel porous supports in air is necessary in order to create a Fe-Cr oxide layer. This layer allows a better adhesion between the support and the ceramic layer, thus reducing at the same time the possibilities of inter-metallic diffusion of Pd [12,18]. Finally, the

main techniques for the deposition of a Pd-based layer are electroless plating (ELP), electroplating, physical vapor deposition (PVD) and chemical vapor deposition (CVD) [19].

The use of Pd-based supported membranes in FBMRs has received a growing interest in the last decade [20–24]. However, the long-term stability of the membranes in fluidized bed membrane reactors at high temperatures (> 400 °C) is limited, since defects can appear due to the mobility of the atoms present in the selective layer or as consequence of the attrition by the fluidized particles. To overcome the stability problems of membranes in fluidized beds, this work focuses on the development of novel double-skin membranes, which offer attrition resistance under fluidization conditions thanks to the addition of a very thin porous ceramic protective layer on top of the Pd-based H_2 perm-selective layer.

In particular, a conventional metallic-supported membrane and a counterpart double-skin (DS) membrane have been tested under fluidization conditions and their performance has been compared to investigate the long-term stability of the novel DS membranes. It was found that in the temperature range of 400-500 °C, conventional supported membranes suffer from a pronounced decay in the initial ideal H_2/N_2 perm-selectivity in the presence of the fluidized catalyst, whereas the novel DS-membranes maintain much higher selectivities at the same conditions. In the first part, the preparation of the membranes, and the characterization techniques and experimental setup used for the tests are described. Subsequently, the main findings are presented and discussed in the results section, and finally the main conclusions of this work are summarized.

2. Experimental

2.1. Membrane preparation

Porous Hastelloy X tubes with media grade of 0.2 μm, welded to non-porous Inconel tubes at both ends (having one side as dead-end) from Mott Metallurgical Corporation have been used in this work as membrane support material. The supports have an outer diameter of 3/8'' and an active (porous) length of 139 mm.

Before the deposition of the ceramic barriers, the metallic supports were oxidized at 750 °C for 1 hour with a heating rate of 3 °C min^{-1}. In order to decrease the pore size and roughness at the

surface, the supports were graded with α-Al_2O_3/YSZ and YSZ slurries before the deposition of the Pd-Ag layer. The slurry of the ceramic barrier consisted of α-Al_2O_3 particles (AKP-30, Sumitomo) and YSZ (TZ-8Y, Tosoh Corp.) particles dispersed in deionized water. Then, polyvinyl alcohol (PVA, MW 78000 g mol^{-1}, Polyscience Europe Gmbh) solution and polyethylene glycol (PEG 400 g mol^{-1} synthesis grade, Scharlau) were added to the slurries. The composition of the slurries used in this work are summarized in Table 1.

Table 1. Components of the inter-diffusion barrier slurries.

Material	Concentration at the slurry (wt. %)	
	Slurry A	Slurry B
α-Al_2O_3	2.1	0
YSZ	0.9	1.5
PVA	3	1.5
PEG	0.6	0.3

The metallic porous supports were dipped into the slurry for 3 minutes at 25 °C, and were subsequently dried in a climatic chamber under continuous rotation for 5 h at 40 °C and 60 % relative humidity. Finally, the samples calcined in air at 400 °C for 30 minutes in order to decompose the organics present at the slurry and then sintered at 750 °C for 4 hours in a 10 %vol. H_2 in He atmosphere. After each sintering process, and prior to the next coating, the roughness and the nitrogen permeance of the supports were measured. In total five coatings were performed (3 of slurry A followed by 2 coatings of slurry B) for membrane M15 and three coatings for M33 (2 of slurry A followed by a single coating of slurry B). A final sintering treatment has been performed during 6 hours at 800 °C under the H_2/He atmosphere.

The deposition of the Pd-Ag layer was carried out by a simultaneous electroless plating technique (ELP). First, the surface of the porous substrate was activated with palladium seeds by dipping the membrane into a chloroform solution of palladium acetate. This step has been repeated 6 times. Subsequently, the membranes were dried at 110 °C and the palladium seeds were reduced in a hydrazine solution at room temperature. Finally, the tubes were cleaned with water and dried again. This cycle was repeated until the surface turned to a homogeneous black color. The Pd-Ag co-deposition has been performed at 64 °C for 5 hours. During the first 2 hours, the membranes were rotating inside the bath and in the last 3 hours vacuum was applied from inside the tube. The deposition time and the composition of the bath used for the

preparation of the two membranes (M15 and M33) are summarized in Table 2. As the last step of the process, the membranes were cleaned, dried and annealed at 650 °C for 4 hours in a reducing atmosphere.

Table 2. Chemical composition of electroless plating bath and deposition time for membranes M15 and M33.

Parameter	M15	M33
Palladium acetate (M)	0.0103	0.0122
Silver nitrate (M)	$7.5 \cdot 10^{-4}$	$3 \cdot 10^{-4}$
EDTA (M)	0.15	0.15
Ammonia (M)	5	5
Hydrazine (M)	0.015	0.015
Deposition time (min)	309	323

The membrane M15 has been first investigated as prepared, and subsequently it has been turned into a double skinned membrane. To do so, a mesoporous YSZ/γ-Al_2O_3 protecting layer has been deposited on top of the Pd-Ag layer of membrane M15 by a vacuum-assisted dip-coating technique at room temperature, followed by calcination at 550 °C for 4 hours [25]. The protective layer containing 50 wt. % of YSZ is expected to be ~ 1 µm-thick, as reported in a previous work [26]. The membrane M15 with the protective layer is henceforth named as M15-DS. The colors present at the surface of the membrane (see Figure 1) is associated with the scattered visible light by the YSZ particles present at the mesoporous protective layer.

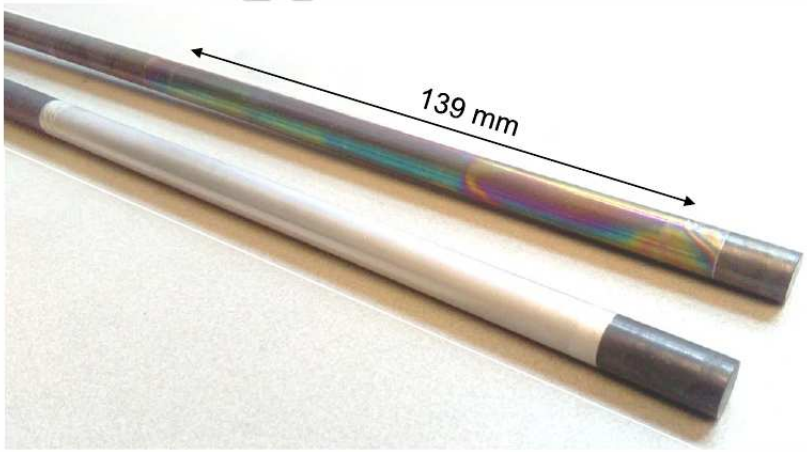

Figure 1. A Pd-Ag double-skinned membrane with a ceramic protective layer supported onto a Hastelloy X porous support (up) and a conventional supported membrane (down).

2.2. Membrane characterization

Prior to the deposition of the selective Pd-Ag layer, the surface roughness (R_a and R_t) and the nitrogen permeance of the metallic porous supports have been determined after each deposition step in the membrane preparation process. The surface roughness was analyzed with a Vecco Dektak 150 contact profilometer, and the measurement has been done using a 2 μm radius stylus tip. After each deposition step, the measurement has been performed at five different locations with a spot length of 4 mm long. The R_t is the total height of the roughness profile (highest peak to valley distance) and R_a is the arithmetical mean roughness.

The composition of the selective layer was determined by measuring the concentration of both metals (Pd and Ag) in the plating bath before and after the deposition of the layer with an ICP-OES technique in a Varian Vista MPX Inductively Coupled Plasma Optical Emission Spectrometer.

The thickness of the deposited ceramic layer and the perm-selective layers has been determined by scanning electron microscope (SEM) techniques in a FEI Quanta 250 FEG equipment. These measurements were carried out using a metallic supported membrane prepared using exactly the same conditions as M15.

2.3. Gas permeation measurements

The membranes were installed in a reactor made of stainless steel (AISI310) with an inner diameter of 102 mm and 100 cm in height, with a porous plate distributor (40 μm pore size) welded at the bottom. A more detailed description of the setup used for permeation tests can be found in the work of Helmi et al. [22]. First, the permeation properties of membrane M15 (without the protective layer) were determined at 500 °C in an empty reactor. Then, the protective layer was deposited onto this membrane and finally both membranes (M15-DS and M33) were installed in the reactor. The system was heated under a nitrogen atmosphere up to 400 °C at a heating rate of 2 °C min^{-1}. Before the investigation into the performance of the membranes, they were activated in air at 400 °C for two minutes in order to remove organic impurities from the surface. Afterward, the nitrogen and hydrogen single gas permeation measurements were carried out at temperatures between 400 and 500 °C. The activation energy

for hydrogen permeation was calculated from the hydrogen permeation values at various temperatures by fitting Sieverts' law, as reported previously [26]. Subsequently, the module was cooled down to room temperature in order to integrate the catalyst particles inside the reactor. The particles used consisted of modified alumina particles with 0.5 wt.% of rhodium with a particle size ranging between 100 and 300 μm provided by Johnson Matthey® (typical catalyst for methane reforming in fluidized beds). The performance of the membranes was monitored for 615 h in the presence of the catalyst in the continuous bubbling fluidization regime at 400-500 °C.

3. Results and discussion

3.1. Membrane characterization

As described in the previous section, α-Al_2O_3-YSZ and YSZ layers have been deposited onto the metallic porous substrates prior to the deposition of the Pd-Ag layer to avoid a possible interaction between metallic elements present in the supports and the selective layer at high temperatures. After each deposition of ceramic barrier, the roughness (R_a and R_t) of the supports has been determined and the values measured are listed in Table 3. The initial R_t of the porous supports (~ 8.1 μm) decreases for both membranes, M15 and M33, after each deposition. After the deposition of a layer with slurry A (α-Al_2O_3, YSZ), the R_t of M15 decreases to almost half of the initial R_t (~ 4.15 μm), while membrane M33 required the deposition of 5 layers to reach similar values. A similar trend is observed for the R_a parameter, which largely decreased after the first deposition for M15, but decreased much less pronounced after subsequent depositions.

The nitrogen permeance has been measured after each deposition of a ceramic layer. The decay in the nitrogen permeance after the first layer deposition, $1.02 \cdot 10^{-5}$ mol m^{-2} s^{-1} Pa^{-1} for M15 and $2.46 \cdot 10^{-5}$ mol m^{-2} s^{-1} Pa^{-1} for M33 corresponds to the decrease in surface roughness. Before the deposition of the Pd-Ag layer, the nitrogen permeances are around 5.7 (M15) and 3.7 (M33) times smaller than the nitrogen permeance of the bare tubes.

Finally, the ELP deposition of the Pd-Ag layer was carried out for 303 min and 328 min onto M15 and M33 respectively and the determined nitrogen permeances were for both lower than $7 \cdot 10^{-10}$ mol m^{-2} s^{-1} Pa^{-1} after annealing at 550 °C for 4 h.

Table 3. Surface roughness and nitrogen permeances of membranes M15 and M33 after deposition of each ceramic layer and the Pd-Ag layer.

Step	Ra (μm)		Rt (μm)		N_2 permeance[b] (mol m^{-2} s^{-1} Pa^{-1})	
	M15	M33	M15	M33	M15	M33
Support[a]	0.86 ± 0.14		8.10 ± 2.14		$4.71 \cdot 10^{-5}$	
Oxidized[a]	0.88 ± 0.13		8.49 ± 1.32		$3.34 \cdot 10^{-5}$	
Slurry A (1st)	0.56 ± 0.01	0.84 ± 0.13	4.15 ± 0.45	6.46 ± 1.08	$1.02 \cdot 10^{-5}$	$2.46 \cdot 10^{-5}$
Slurry A (2nd)	0.48 ± 0.02	0.72 ± 0.13	4.08 ± 0.76	5.67 ± 1.78	$9.68 \cdot 10^{-6}$	$2.03 \cdot 10^{-5}$
Slurry A (3rd)	-	0.67 ± 0.12	-	4.35 ± 0.66	-	$1.82 \cdot 10^{-5}$
Slurry B (1st)	0.44 ± 0.05	0.61 ± 0.06	4.19 ± 0.95	5.71 ± 2.44	$8.22 \cdot 10^{-6}$	$1.86 \cdot 10^{-5}$
Slurry B (2nd)	-	0.63 ± 0.14	-	4.70 ± 1.49	-	$1.42 \cdot 10^{-5}$
Final sintering	NA	0.59 ± 0.08	NA	4.09 ± 0.58	NA	$1.27 \cdot 10^{-5}$
ELP[c]	-	-	-	-	$6.55 \cdot 10^{-10}$	$1.70 \cdot 10^{-11}$

NA: not available data
[a] Average values from other five bare supports
[b] Measured at room temperature.
[c] after annealing at 650 °C for 4 hours

SEM cross section images were obtained from another metallic supported membrane prepared under the same conditions as M15. As can be observed in Figure 2 (a and b), the pores of the support (very irregular) ranges between 10 and 20 μm. Furthermore, it has also been observed that the thickness of the ceramic inter-diffusion barrier is not homogeneous along the membrane. In some regions, the ceramic layer creates a barrier between the selective layer and the support pores (Figure 2c), while in other regions this ceramic barrier is not observed (i.e. is very thin) and the selective Pd-Ag layer seems to be deposited directly onto the support surface (Figure 2d). Therefore, inter-diffusion of metallic species from the support towards the selective layer could be expected when working at high temperatures. From Figure 2b and Figure 2c, it can also be confirmed that the pores in the surface of the metallic support are well covered by ceramic particles. The measured average thickness of the Pd-Ag layer from 5 different cross section images was 4.02 μm (± 0.24 μm), and a similar thickness could also be expected for M33. The measured silver content in the selective layer of membrane M33 is lower (~ 6.9% wt. %) than in M15 (~ 16.8 wt. %). This is expected since the amount of silver nitrate added for the electroless plating for M15-DS was 2.5 times larger than for M33, and this is in agreement with the determined silver content measured for both membranes, being 2.43 times larger for M15-DS.

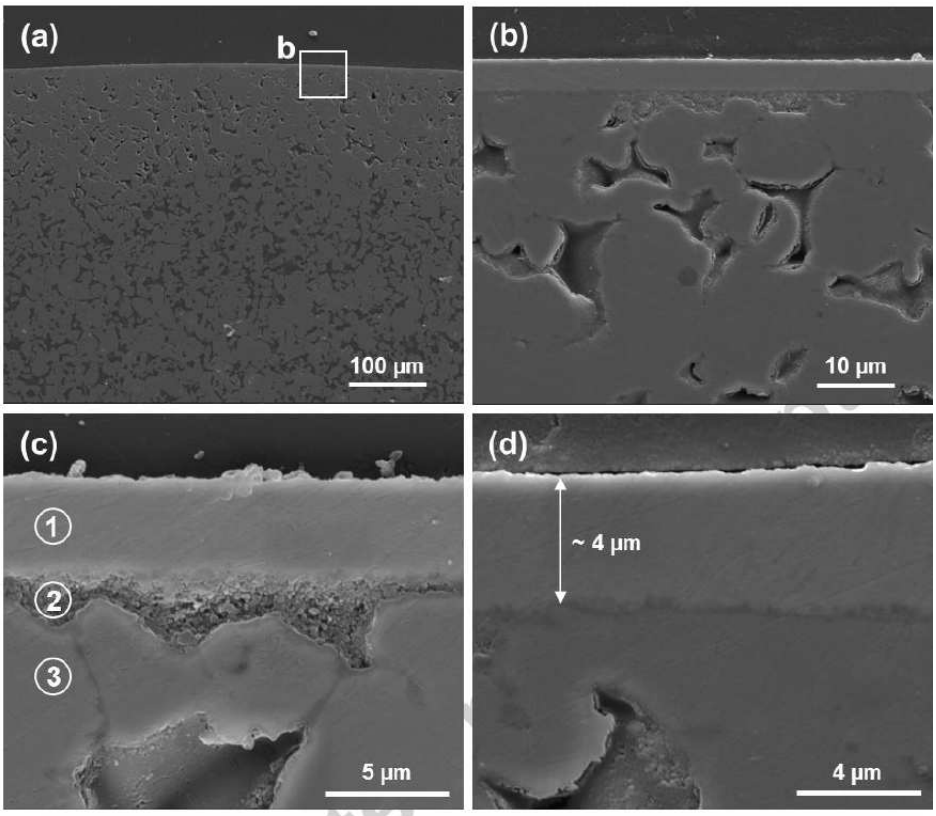

Figure 2. SEM cross section image of a conventional Pd-Ag metallic supported membrane. Images with different magnifications: 250x (a), 2500x (b), 8000x (c) and 10000x (d). Numbered points in (c) are related to the Pd-Ag layer (1), YSZ-Al_2O_3 interdiffusion layer (2) and Hastelloy X porous support (3).

3.2. Membrane permeation properties

The main goal of this test is to compare the permeation properties of a conventional supported Pd-Ag membrane with the new double-skin (DS) membrane before and during fluidized conditions. The metallic supports allow an easier installation of the membranes into the reactor since they can be easily connected to the metallic reactor using standard Swagelok fittings (or, in a real reactor, by welding of the tube to the reactor flange).

Before the deposition of the mesoporous protective layer onto M15, its permeation properties have been measured in pure hydrogen and nitrogen at 500 °C and 3 bar of pressure difference for about 500 h (after activation by flowing diluted air at 500 °C for 1 min). As reported in Figure 3, the hydrogen permeance of the membrane ($1.92 \cdot 10^{-6}$ mol m^{-2} s^{-1} Pa^{-1}) remains stable during the

whole duration of the experiment, while the ideal H_2/N_2 perm-selectivity decays from 3300 to 1700. The nitrogen leakage at 500 °C increased from $5.89 \cdot 10^{-10}$ to $1.19 \cdot 10^{-9}$ mol m^{-2} s^{-1} Pa^{-1} (with a pressure difference of 3 bar). After this test, the leakages of the membrane have been checked by introducing the membrane in ethanol and pressurizing with helium from the inner side of the tube (1 bar of pressure difference). During this test, bubbles coming out from the membrane surface were observed.

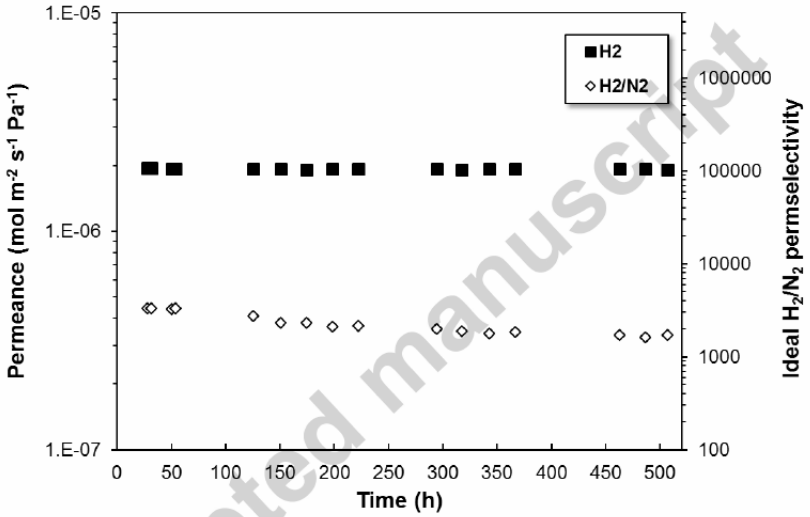

Figure 3. H_2 permeance and ideal H_2/N_2 perm-selectivity of the M15 membrane at 500 °C and 3 bar of pressure difference.

Once the mesoporous layer was deposited onto M15 (from now on referred to as M15-DS) these bubbles were not observed (i.e. the small pores on the membrane surface were covered by ceramic particles, effectively improving the perm selectivity of the membrane). The hydrogen permeation for both membranes (M15-DS and M33) was measured at different transmembrane pressures and at temperatures in the range of 400-500 °C (see Figure 4) after being exposed to air for 2 minutes at 400 °C for their activation. The membranes showed a linear trend with a pressure exponential factor, n, of 0.62 and 0.72 for M33 and M15-DS respectively. It is well accepted that the deviation from the Sieverts' law (n=0.5) can be attributed to the influence of the support or to external mass transfer limitations [27,28]. The addition of the mesoporous protective layer leads to an increase in the n-value, which could be related to the effects of

Knudsen diffusion and viscous flow in the porous protective layer, as reported in a previous work [26].

The activation energies determined for the temperature range of 400-500 °C are 6.26 and 7.17 kJ mol^{-1} for M15-DS and M33, respectively. An activation energy and n-value of 5.8 kJ mol^{-1} and 0.738, respectively, was reported by Fernandez et al. [29] for a membrane with 4-5 µm-thick Pd-Ag layer supported onto a Hastelloy-X porous substrate using the same ceramic interdiffusion barrier as reported in this work. The lower activation energy of M15-DS in comparison with M33 can be attributed to the effect of the Knudsen-viscous diffusion through the mesoporous protective layer, where this diffusion mechanism is characterized by a lower activation energy than the solution-diffusion mechanism in the Pd-Ag selective layer [30].

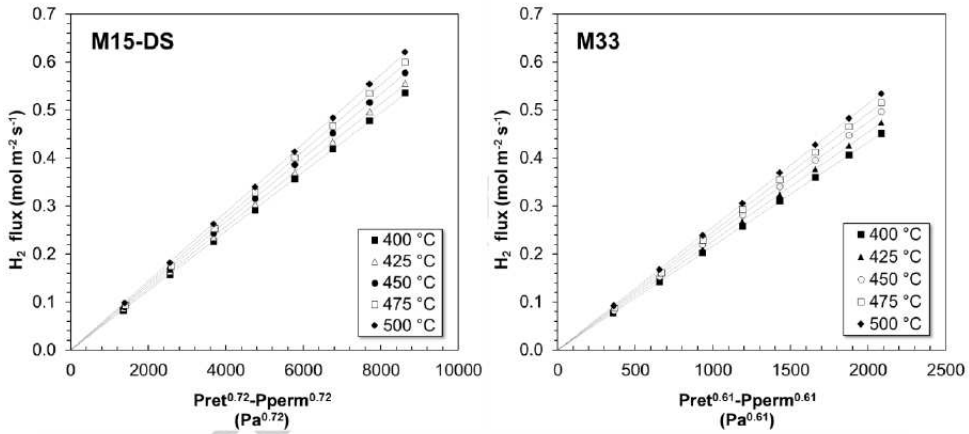

Figure 4. Measured hydrogen flux from 400 °C to 500 °C after activation in air at 400 °C as a function of the hydrogen pressure difference.

The main parameters obtained during the single gas permeation test for the conventional and double-skinned membranes are summarized in Table 4. The results show that the hydrogen permeance of M15-DS at 500 °C ($1.55 \cdot 10^{-6}$ mol m^{-2} s^{-1} Pa^{-1}) is somewhat lower than for M15 ($1.92 \cdot 10^{-6}$ mol m^{-2} s^{-1} Pa^{-1}), which was expected due to the presence of the mesoporous protective layer that increases the mass transfer resistance. A slightly lower permeance ($1.34 \cdot 10^{-6}$ mol m^{-2} s^{-1} Pa^{-1}) was measured for the metallic supported membrane M33, which could be related to the lower content in silver in comparison with M15-DS, as mentioned previously. It is indeed already reported in the literature that the addition of Ag to Pd improves the hydrogen

permeability, resulting in a 1.7 times larger permeation rate when 23 wt.% of silver is added compared to pure palladium [31]. On the other hand, no nitrogen flow was detected using a Bronkhorst flow meter (0.001 mL min^{-1}) through the double-skinned membrane, resulting in a virtually infinite perm-selectivity. For graphical purposes, the nitrogen permeation selected is that of the detection limit of the flow meter, leading to a N_2 permeance of $4.47 \cdot 10^{-13}$ mol m^{-2} s^{-1} Pa^{-1} at 4 bar of transmembrane pressure and to an ideal perm-selectivity of 3500000. For membrane M33, the ideal selectivity measured was 93300, corresponding to a nitrogen leakage of $1.43 \cdot 10^{-11}$ mol m^{-2} s^{-1} Pa.

Table 4. Main parameters of conventional metallic supported (M33) and double-skin membrane (M15-DS) in an empty reactor.

Parameters	M15-DS	M33
H_2 permeance (mol m^{-2} s^{-1} Pa^{-1})*	$1.55 \cdot 10^{-6}$	$1.34 \cdot 10^{-6}$
Ideal H_2/N_2 perm-selectivity*	> 3500000	93300
Ea (kJ mol^{-1})	6.26	7.17
n-value	0.72	0.61

*Measured at 500 °C and ΔP = 4 bar.

3.3. Long-term membrane performance under catalyst fluidization

After 200 hours of the preliminary test (single gas test in an empty reactor), the system was cooled down to room temperature for the addition of the catalyst particles into the reactor (first peak in the temperature profile in Figure 5). Once more, the system was heated to 400 °C while catalyst particles were kept under continuous bubbling fluidization. The particle size of the catalyst is 170 micron, the minimum fluidization velocity measured in N2 is 0.014 m/s and 0.011 m/s at 400 and 500 °C, respectively. The tests were carried out at velocities between 3 and 5 u/umf. The membrane stability under fluidization conditions has been evaluated between 400 and 500 °C for a total time of 615 hours (115 at 400 °C and 500 hours at 500 °C). The main objective of this test is to compare the performance and long-term stability of the two membranes under fluidization conditions. As shown in Figure 5, once the catalyst was filled in the reactor, the ideal perm-selectivity of the conventional supported membrane (M33) decreased during the first hours to ~14000. This value further decreased until ~1000 after 615 hours, caused by an increase in the nitrogen leakage from $8.76 \cdot 10^{-11}$ to $1.4 \cdot 10^{-9}$ mol m^{-2} s^{-1} Pa^{-1} at 4 bar of pressure difference. On the other hand, the DS-membrane (M15-DS) did not show any nitrogen

leakage under the same conditions, demonstrating indeed a much higher attrition resistance than the conventional metallic supported membrane. In terms of H_2 permeance stability, the H_2 permeance of membrane M33 has been progressively increasing during the test, while the double-skin membrane suffered from a small decrease in time, which can be associated with some sintering of the protective layer and/or an interaction between the gamma-alumina and palladium layers. Densification of the protective layer can occur during the fluidization test at 500 °C, decreasing the pore size and thus the H_2 permeance of the overall membrane. Interaction between support and palladium was observed by Pacheco Tanaka et al at 650 °C were the hydrogen flux decay about 50 % after 130 hours, while not decay was observed at 550 °C. However, the support was made by α-Al_2O_3 instead of γ-Al_2O_3 (the case in this work) which may interact with palladium at lower temperatures than α-Al_2O_3. The sintering of the ceramic interdiffusion barrier does not seem to be responsible of this decrease in the permeance, since M15 was tested at 500 °C for ~ 500 hours without showing any flux decay (Figure 3). Nonetheless, it was observed that during the last 200 hours at 500 °C the hydrogen permeance of both membranes reached a plateau with values of $1.20 \cdot 10^{-6}$ and $1.43 \cdot 10^{-6}$ mol m^{-2} s^{-1} Pa^{-1} for M15-DS and M33, respectively. During the test in the bubbling fluidization regime, the setup was cooled down twice as can be observed in the temperature profile of Figure 5. No effect on the H_2 permeance was observed, concluding that the leakage of both membranes did not increase as a result of these temperature changes.

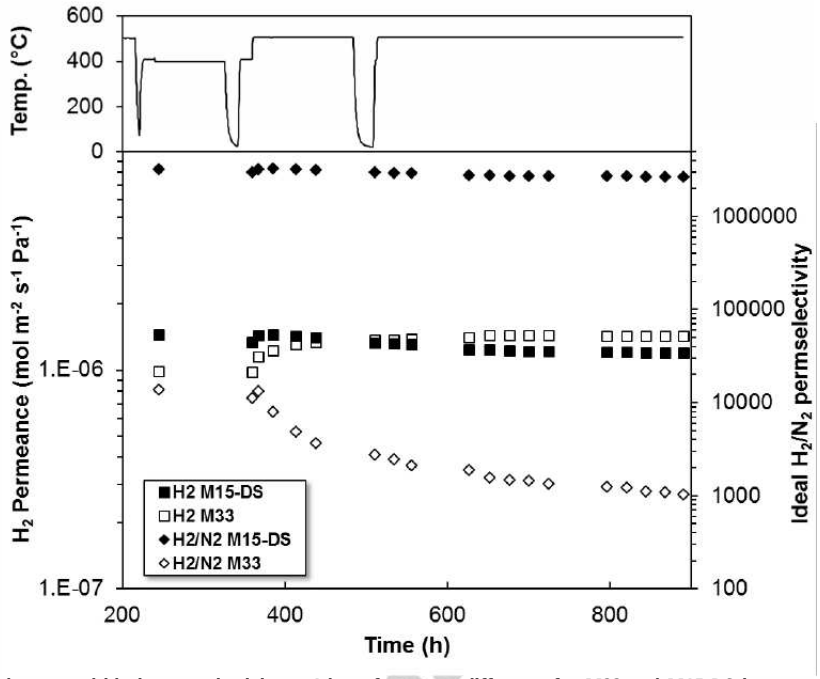

Figure 5. Hydrogen and ideal perm-selectivity at 4 bar of pressure difference for M33 and M15-DS in presence of Rh based catalyst under bubbling fluidization conditions.

Only a few reports on long term stability of Pd membranes under fluidization conditions have been reported so far. The characteristic of the membranes, particles, operating conditions and their permeation properties (permeance and ideal selectivity) reported so far in the literature are summarized in Table 5.

The initial ideal perm-selectivity of membranes prepared onto alumina supports is, in general, lower than metallic supported membranes. For alumina-supported membranes, the largest selectivity was found to be around 27000, which decreased down to 10000 after 48 hours at 400 °C under continuous fluidization with alumina-based particles [32]. A better performance was observed after 600 h at 400 °C by Helmi et al. [22]. These authors observed a drop in the ideal perm-selectivity (from 20000 to 13000), which was caused by a thermal shock that the membrane module suffered due to an oven failure during the test. A ceramic supported double-skin membrane showed a decrease in the selectivity from 25000 to 5000 after 750 hours of fluidization with glass beads at 350-400 °C [26]. After the test, it was found that the protective layer was pealed off, which was attributed to the softening of the glass beads and subsequent

adhesion to the protective layer, which was then finally removed due to the collision of these particles with other particles of the fluidized bed. A similar membrane (showing a defect prior to the test) was tested at 400 °C with alumina particles, and the selectivity remained constant (~ 2000) over 1500 hours. Only when the temperature was increased, a decrease in the selectivity was observed and this was attributed to a sealing failure. A faster sealing failure was observed for another ceramic-supported DS membrane also referred to in [26] and tested at higher temperatures (550 °C) for 700 hours. Similar sealing problems were also observed by other authors when employing ceramic supports for the preparation of the H_2 selective membrane [33]. On the other hand, when metallic supports are used, the sealing problems are avoided and the performance of the membrane alone can be evaluated under fluidization conditions. Roses et al. [24] reported the performance of a Pd-Ag membrane supported onto an Inconel porous tube (one selective layer on the outer surface and another one on the inner surface of the tube), and no leakages were observed during 260 hours of continuous fluidization. A membrane prepared in the same way as M33 was tested by Medrano et al. [21] and showed an ideal selectivity of >200000 for about 800 hours in an empty reactor, while this selectivity decreased to 2850 at 600 °C. The authors attributed the increased leakage to a defect formation in the surface of the membrane. Later, the membrane was tested under reactive conditions in a fluidized bed membrane reactor in the temperature range of 500-600 °C. However, the performance in terms of perm-selectivity was quite low (< 600) in comparison to M33. Finally, as mentioned previously, the addition of the protective layer allows preventing attrition and a high ideal perm-selectivity was maintained. The M15-DS did not show any leakages and the calculated perm-selectivity remained close to 3 million. The selectivity decrease suffered along the 615 hours test, is related to the previously mentioned H_2 flux reduction. Two other works have been reported using the same type membrane as M33 [34,35]. Medrano et al. [34] reported on the demonstration of the MA-CLR (membrane assisted chemical looping reforming) using three metallic-supported membranes and found that the ideal perm-selectivity decreased from 5400 to 4850 after 100 hours of operation at 500-600 °C. A longer test was reported by Wassie et al. [35] for a different concept, viz. MA-GSR (membrane assisted gas switching reforming), where four membranes were tested for about 240 hours at temperatures ranging from 400 to 550 °C. However, their initial perm-selectivity (11000) decreased down to merely 150, which was

attributed to defect formation at the membrane surface due to the formation of PdO resulting in the formation of pores in the selective layer.

These results demonstrate that the double-skin membranes exhibit a much better performance under fluidization conditions than other supported membranes. Future work will be focused on the evaluation of the performance of the double skin membranes under reactive conditions.

Table 5. Permeation properties of Pd-based supported membranes in a fluidized bed membrane reactor reported in the literature.

Selective layer/ support	Thickness selective layer (μm)	Particles	Temp. (°C)	ΔP (bar)	H_2 permeance (10^{-6} mol m^{-2} s^{-1} Pa^{-1})	Test duration (h)	H_2/N_2		Ref.
							t=0	t=end	
$PdAg/Al_2O_3$	3-4	Pt-$Ni/CeO_2/SiO_2$	450-550	1.5-3	1.25[f]	~ 500	~1290[f]	N/A	[33]
$PdAg/Al_2O_3$	1.29	Pt/Al_2O_3	400	1	9	1000	1800	1600	[20]
YSZ-Al_2O_3/PdAg/Al_2O_3	1	Glass beads	350-400	1	4.6	750	~ 25000	~ 5000	[26]
YSZ-Al_2O_3/PdAg/Al_2O_3	1-2	Rh/Al_2O_3	400-500	1	3.35	2000	2000	100	[26]
YSZ-Al_2O_3/PdAg/Al_2O_3	1.86	Rh/Al_2O_3	550	1	1.3	700	1500	50	[26]
$PdAg/Al_2O_3$	3.6	Al_2O_3[b]	400	1-4	5	48	27000	10000	[32]
$PdAg/Al_2O_3$	4-5	Pt/Al_2O_3	400	1	4	600	20000	13000	[22]
PdAg/PSS	25	NiO/Al_2O_3	550	6.5-9.7	0.4-0.8[e]	178	~ 3000[d]	~1700[d]	[23]
PdAg/Inconel/PdAg	4.5[a]	Al_2O_3[b]	500-630	5.2	N/A	260	∞	∞	[24]
PdAg/Hast. X	4-5	$NiO/CaAl_2O_4$	500-600	1-4	1.3	-	574	132	[21]
PdAg/Hast. X	4-5	$NiO/CaAl_2O_4$	500-600	1	1.3	100	5400	4890	[34]
PdAg/Hast. X	4-5	NiO/Al_2O_3	400-550	1-2	0.8	240	10000	150	[35]
PdAg/Hast. X	4	Rh/Al_2O_3	400-500	4	1.2	615	14000	1000	This work
YSZ-Al_2O_3/PdAg/Hast. X	4	Rh/Al_2O_3	400-500	4	1.43	615	3500000	2700000[c]	This work

N/A: Not available or not reported by authors.
[a] 2 layers of PdAg, the one in the ourter surface has a thickness of 3 μm and the one oin the inner side of 1.5 μm.
[b] Alumina particles as a filler together with a noble metal-based CPO catalyst
[c] The used nitrogen permeance for the calculation of ideal permselectivity was based in the detection limit of the flow meter (0.001 mL min^{-1}).
[d] The real selectivity has been calculated Taking into account the measured H_2 purity at the permeate under reactive conditions for the experiment number 4 (99.995) and experiment number 16. (99.94 %)

[e] Permeated hydrogen for experiment 4 and 6. H_2 permeance was calculated while taken into account the installed membrane area and pressure difference between retentate and permeate sides.
[f] Average value for 5 membranes

4. Conclusions

In this paper, two different Pd-Ag membranes supported on porous metallic supports have been prepared, tested and characterized. The objective of this work was to investigate the performance of these membranes against attrition when they are immersed in fluidized beds. Porous metallic supports have been employed in this work due to their higher mechanical strength in comparison to porous ceramic supports. The addition of a porous protective layer (the so-called double-skin membrane) to a Pd-Ag layer largely enhanced the stability of the performance of membranes under fluidization conditions, paving the way for their application in fluidized bed membrane reactors. In fact, it was observed that the membrane without the protective layer suffered from significant erosion leading to an increase in the nitrogen leakage under fluidization conditions, while the performance of the double-skin membrane remained stable for more than 615 hours at temperatures of 400-500 °C and at 4 bar of pressure difference. The high ideal perm-selectivity measured with the double-skin membrane achieves the H_2 purity needed for its use in fuel cells, which could promote the further development of membrane reactors for small-scale hydrogen production. The results of this paper also clearly show that the protective layer can be used to improve the perm-selectivities of membranes that have small defects on their surface.

Acknowledgements

The presented work is funded within FERRET project as part of European Union's Seventh Framework Programme (FP7/2007-2013) for the Fuel Cells and Hydrogen Joint Technology Initiative under grant agreement n. 621181. Note: "The present publication reflects only the authors' views and the Union is not liable for any use that may be made of the information contained therein".

Bibliography

[1] Y.N. Wang, A.E. Rodrigues, Hydrogen production from steam methane reforming coupled with in situ CO2capture: Conceptual parametric study, Fuel. 84 (2005) 1778–1789. doi:10.1016/j.fuel.2005.04.005.

[2] S.Z. Abbas, V. Dupont, T. Mahmud, Kinetics study and modelling of steam methane reforming process over a NiO/Al2O3catalyst in an adiabatic packed bed reactor, Int. J. Hydrogen Energy. 42 (2017) 2889–2903. doi:10.1016/j.ijhydene.2016.11.093.

[3] F. Gallucci, E. Fernandez, P. Corengia, M. van Sint Annaland, Recent advances on membranes and membrane reactors for hydrogen production, Chem. Eng. Sci. 92 (2013) 40–66. doi:10.1016/j.ces.2013.01.008.

[4] G.S. Burkhanov, N.B. Gorina, N.B. Kolchugina, N.R. Roshan, D.I. Slovetsky, E.M. Chistov, Palladium-based alloy membranes for separation of high purity hydrogen from hydrogen-containing gas mixtures, Platin. Met. Rev. 55 (2011) 3–12. doi:10.1595/147106711X540346.

[5] C.S. Patil, M. van Sint Annaland, J.A.M. Kuipers, Fluidised bed membrane reactor for ultrapure hydrogen production via methane steam reforming: Experimental demonstration and model validation, Chem. Eng. Sci. 62 (2007) 2989–3007.

[6] A. Arratibel, D.A.P. Tanaka, M. van Sint Annaland, F. Gallucci, Membrane reactors for autothermal reforming of methane, methanol, and ethanol, 2015. doi:10.1016/B978-1-78242-223-5.00003-0.

[7] A. Arratibel Plazaola, D.A. Pacheco Tanaka, M. van Sint Annaland, F. Gallucci, Recent advances in Pd-based membranes for membrane reactors, Molecules. 22 (2017) 1–53. doi:10.3390/molecules22010051.

[8] A. Tardini, C. Gerboni, L. Cornaglia, PdAu membranes supported on top of vacuum-assisted ZrO2-modified porous stainless steel substrates, J. Memb. Sci. 428 (2013) 1–10. doi:10.1016/j.memsci.2012.10.029.

[9] S.-K. Ryi, S.-W. Lee, D.-K. Oh, B.-S. Seo, J.-W. Park, J.-S. Park, D.-W. Lee, Electroless plating of Pd after shielding the bottom of planar porous stainless steel for a highly stable Hydrogen selective membrane, J. Memb. Sci. (2014). doi:10.1016/j.memsci.2014.04.058.

[10] F. Braun, A.M. Tarditi, J.B. Miller, L.M. Cornaglia, Pd-based binary and ternary alloy membranes: Morphological and perm-selective characterization in the presence of H2S, J. Memb. Sci. 450 (2014) 299–307. doi:10.1016/j.memsci.2013.09.026.

[11] H. Gao, J. Slin, Y. Li, B. Zhang, Electroless plating synthesis, characterization and permeation properties of Pd–Cu membranes supported on ZrO2 modified porous stainless steel, J. Memb. Sci. 265 (2005) 142–152. doi:10.1016/j.memsci.2005.04.050.

[12] K. Zhang, H. Gao, Z. Rui, P. Liu, Y. Li, Y.S. Lin, High-Temperature Stability of Palladium Membranes on Porous Metal Supports with Different Intermediate Layers, Ind. Eng. Chem. Res. 48 (2009) 1880–1886. doi:10.1021/ie801417w.

[13] Y. Huang, R. Dittmeyer, Preparation and characterization of composite palladium membranes on sinter-metal supports with a ceramic barrier against intermetallic diffusion, J. Memb. Sci. 282 (2006) 296–310. doi:10.1016/j.memsci.2006.05.032.

[14] C.-B. Lee, S.-W. Lee, J.-S. Park, S.-K. Ryi, D.-W. Lee, K.-R. Hwang, S.-H. Kim, Ceramics used as intermetallic diffusion barriers in Pd-based composite membranes sputtered on porous nickel supports, J. Alloys Compd. 578 (2013) 425–430. doi:10.1016/j.jallcom.2013.06.007.

[15] M. Chotirach, S. Tantayanon, S. Tungasmita, K. Kriausakul, Zr-based intermetallic diffusion barriers for stainless steel supported palladium membranes, J. Memb. Sci. 405–406 (2012) 92–103. doi:10.1016/j.memsci.2012.02.055.

[16] A. Calles, D. Alique, L. Furones, Thermal stability and effect of typical water gas shift reactant composition on H2 permeability through a Pd-YSZ-PSS composite membrane, Int. J. Hydrogen Energy. 39 (2014) 1398–1409. doi:10.1016/j.ijhydene.2013.10.168.

[17] G. Straczewski, J. Völler-Blumenroth, H. Beyer, P. Pfeifer, M. Steffen, I. Felden, A. Heinzel, M. Wessling, R. Dittmeyer, Development of thin palladium membranes supported on large porous 310L tubes for a steam reformer operated with gas-to-liquid fuel, Chem. Eng. Process. Process Intensif. 81 (2014) 13–23. doi:10.1016/j.cep.2014.04.002.

[18] S. Samingprai, S. Tantayanon, Y.H. Ma, Chromium oxide intermetallic diffusion barrier for palladium membrane supported on porous stainless steel, J. Memb. Sci. 347 (2010) 8–16. doi:10.1016/j.memsci.2009.09.058.

[19] S. Yun, S. Ted Oyama, Correlations in palladium membranes for hydrogen separation: A review, J. Memb. Sci. 375 (2011) 28–45. doi:10.1016/j.memsci.2011.03.057.

[20] J. Melendez, E. Fernandez, F. Gallucci, M. van sint Annaland, P.L. Arias, D.A. Pacheco Tanaka, Preparation and characterization of ceramic supported ultra-thin (~1 μm) Pd-Ag membranes, J. Memb. Sci. 528 (2017) 12–23.

[21] J.A. Medrano, E. Fernandez, J. Melendez, M. Parco, D.A.P. Tanaka, M. van Sint Annaland, F. Gallucci, Pd-based metallic supported membranes: High-temperature stability and fluidized bed reactor testing, Int. J. Hydrogen Energy. (2015) 1–13. doi:10.1016/j.ijhydene.2015.10.094.

[22] A. Helmi, E. Fernandez, J. Melendez, D. Pacheco Tanaka, F. Gallucci, M. van Sint Annaland, Fluidized Bed Membrane Reactors for Ultra Pure H2 Production—A Step forward towards Commercialization, Molecules. 21 (2016) 376. doi:10.3390/molecules21030376.

[23] A. Mahecha-Botero, T. Boyd, A. Gulamhusein, N. Comyn, C.J. Lim, J.R. Grace, Y. Shirasaki, I. Yasuda, Pure hydrogen generation in a fluidized-bed membrane reactor: Experimental findings, Chem. Eng. Sci. 63 (2008) 2752–2762.

[24] L. Roses, F. Gallucci, G. Manzolini, M. van Sint Annaland, Experimental study of steam methane reforming in a Pd-based fluidized bed membrane reactor, Chem. Eng. J. 222 (2013) 307–320. doi:10.1016/j.cej.2013.02.069.

[25] A. Arratibel, U. Astobieta, D.A. Pacheco Tanaka, M. van Sint Annaland, F. Gallucci, N2, He and CO2 diffusion mechanism through nanoporous YSZ/γ-Al2O3 layers and their use in a pore-filled membrane for hydrogen membrane reactors, Int. J. Hydrogen Energy. 41 (2016) 8732–8744.

[26] A. Arratibel, A. Pacheco Tanaka, I. Laso, M. van Sint Annaland, F. Gallucci, Development of Pd-based double-skinned membranes for hydrogen production in fluidized bed membrane reactors, J. Memb. Sci. 550 (2017) 536–544. doi:10.1016/j.memsci.2017.10.064.

[27] T. a. Peters, M. Stange, R. Bredesen, On the high pressure performance of thin supported Pd–23%Ag membranes—Evidence of ultrahigh hydrogen flux after air treatment, J. Memb. Sci. 378 (2011) 28–34.

[28] S.K. Ryi, J.S. Park, S.H. Kim, S.H. Cho, D.W. Kim, The effect of support resistance on the hydrogen permeation behavior in Pd-Cu-Ni ternary alloy membrane deposited on a porous nickel support, J. Memb. Sci. 280 (2006) 883–888. doi:10.1016/j.memsci.2006.03.007.

[29] E. Fernandez, J.A. Medrano, J. Melendez, M. Parco, J.L. Viviente, M. van Sint Annaland, F. Gallucci, D.A. Pacheco Tanaka, Preparation and characterization of metallic supported thin Pd-Ag membranes for hydrogen separation, Chem. Eng. J. 305 (2016) 182–190.

[30] X. Tan, K. Li, Dense Metallic Membrane Reactors, in: Inorg. Membr. React. Fundam. Appl., John Wiley and Sons, 2015: pp. 1–290. doi:10.1002/9781118672839.

[31] A. Basile, A. Iulianelli, T. Longo, S. Liguori, M. De Falco, Chapter 2 Pd-based Selective

Membrane State-of-the Art, in: M. De Falco, L. Marrelli, G. Iaquaniello (Eds.), Membr. React. Hydrog. Prod. Process., Springer London, London, 2011. doi:10.1007/978-0-85729-151-6.

[32] E. Fernandez, A. Helmi, K. Coenen, J. Melendez, J.L. Viviente, D.A. Pacheco Tanaka, M. van Sint Annaland, F. Gallucci, Development of thin Pd–Ag supported membranes for fluidized bed membrane reactors including WGS related gases, Int. J. Hydrogen Energy. 40 (2015) 3506–3519.

[33] V. Spallina, G. Matturro, C. Ruocco, E. Meloni, V. Palma, E. Fernandez, J. Melendez, A.D. Pacheco Tanaka, J.L. Viviente Sole, M. van Sint Annaland, F. Gallucci, Direct route from ethanol to pure hydrogen through autothermal reforming in a membrane reactor: Experimental demonstration, reactor modelling and design, Energy. 143 (2018) 666–681. doi:10.1016/j.energy.2017.11.031.

[34] J.A. Medrano, I. Potdar, J. Melendez, V. Spallina, D.A. Pacheco-Tanaka, M. van Sint Annaland, F. Gallucci, The membrane-assisted chemical looping reforming concept for efficient H2production with inherent CO2capture: Experimental demonstration and model validation, Appl. Energy. 215 (2018) 75–86. doi:10.1016/j.apenergy.2018.01.087.

[35] S.A. Wassie, J.A. Medrano, A. Zaabout, S. Cloete, J. Melendez, D.A.P. Tanaka, S. Amini, M. van Sint Annaland, F. Gallucci, Hydrogen production with integrated CO2capture in a membrane assisted gas switching reforming reactor: Proof-of-Concept, Int. J. Hydrogen Energy. 43 (2018) 6177–6190. doi:10.1016/j.ijhydene.2018.02.040.

Highlights:

- Two different Pd-Ag membranes supported have been prepared and tested in a FBMR.
- Membranes were tested in a FBMR for more than 615 h at 400-500 °C.
- The double-skin membrane show better stability under fluidization conditions.
- Convectional membranes suffer from erosion, thus the H_2/N_2 perm-selectivity decay.